Journal of
Instrumentation

Direct detection of particle radiation with perovskite sensors

To cite this article: G. Tinti *et al* 2025 *JINST* **20** C05028

Published by IOP Publishing for Sissa Medialab

Received: *January 31, 2025*
Accepted: *April 14, 2025*
Published: *May 23, 2025*

7th International Conference Frontiers in Diagnostic Technologies
INFN research center of Frascati, Italy
21–23 October 2024

Direct detection of particle radiation with perovskite sensors

G. Tinti,[a,*] M. Testa,[a] A. De Santis,[a] A. Paoloni,[a] G. Papalino,[a] G. Felici,[a] Z. Chubinidze,[a] F. Matteocci,[b] M. Auf der Maur,[b] S. Rizzato,[c] L. Lo Presti,[c] I. Viola,[d] S. Morganti,[e] C. Rovelli[e] and L. Pancheri[f,g]

[a] *Istituto Nazionale di Fisica Nucleare (INFN), Laboratori Nazionali di Frascati,*
Via E. Fermi 54, I-00044 Frascati, Italy
[b] *CHOSE Centre for Hybrid and Organic Solar Energy,*
Department of Electronic Engineering, University of Rome "Tor Vergata",
via del Politecnico 1, 00133 Rome, Italy
[c] *Department of Chemistry, Università degli Studi di Milano, Via Golgi 19, 20133 Milano, Italy*
[d] *CNR-NANOTEC, Istituto di Nanotecnologia c/o Dip. Fisica, Università "La Sapienza",*
Piazzale A. Moro 2, 00185 Roma, Italy
[e] *INFN Sezione di Roma, c/o Department of Physics, Sapienza Università di Roma,*
P.le Aldo Moro 2, 00185 Rome, Italy
[f] *INFN-TIFPA, Via Sommarive, 14, 38123 Trento, Italy*
[g] *Department of Industrial Engineering, University of Trento, Via Sommarive, 9, 38123 Trento, Italy*

E-mail: `gmtinti@lnf.infn.it`

Abstract: In the past decade, organometal halide perovskite (OMHP) semiconductors have been studied as sensors for ionization radiation and X-ray detectors, beside the well known success as photovoltaic devices. Properties such as simple single crystal growth from low-cost solution processes, high stopping power, defect-tolerance, large mobility-lifetime product and tunable bandgap make OMHP very promising materials for novel detectors. An overview of usage of perovskite for radiation detection of charged particles and electromagnetic radiation will be presented. The results of PEROV INFN project will be shown: OHMP based single crystal devices have been developed and tested with electrons from the Beam Test Facility at INFN Frascati National Laboratories, close to the minimum ionizing energy deposition. The crystal sensor can reach the single particle sensitivity with a bias voltage as low as 5 V. It also shows a good linearity of the response as a function of the number of electrons with a dynamic range of approximately 10^4. Efforts towards the application of OMHP sensors as X-ray detectors will also be also discussed.

Keywords: Materials for solid-state detectors; Solid state detectors; X-ray detectors; Photon detectors for UV, visible and IR photons (solid-state) (PIN diodes, APDs, Si-PMTs, G-APDs, CCDs, EBCCDs, EMCCDs, CMOS imagers, etc)

---

[*] Corresponding author.

https://doi.org/10.1088/1748-0221/20/05/C05028

Contents

1 Introduction to perovskites and the PEROV project 1

2 Bulk single crystal performance 2
  2.1 Minimum ionising particle detection 2
  2.2 X-ray detection 2

3 Further developments 3

1 Introduction to perovskites and the PEROV project

Methylammonium lead bromide ($CH_3NH_3PbBr_3$), commonly referred to as $MAPbBr_3$, is an organometal halide perovskite (OMHP) compound that recently has garnered significant interest as a sensor for radiation detection. Table 1 summarizes the key properties of $MAPbBr_3$ compared to silicon, the standard material used in semiconductor detectors.

Table 1. Comparison between Si and $MAPbBr_3$ physical properties.

Semiconductor	Si	$MAPbBr_3$
Density (g/cm^3)	2.33	3.8
Band gap energy E_g (eV)	1.12 (indirect)	2.24 (direct)
Average energy for e/h creation (eV)	3.65	5.83[a]
electron mobility μ_e (cm^2/V/s)	1450	25–140 [2]
hole mobility μ_h (cm^2/V/s)	500	13–220 [2]
Radiation length X_0 (cm)	9.36	2.33
Z[b]	14	62

[a] The value for $MAPbBr_3$ is extracted from the formula $2 \cdot E_g + 1.43\,\text{eV}$ [1].

[b] For $MAPbBr_3$ the effective atomic number is computed as $Z_{\text{eff}} = \sqrt[n]{f_1 \cdot (Z_1)^n + \ldots + f_k \cdot (Z_k)^n}$, where $n = 2.94$ and f_k is the fraction of the total number of electrons associated to the k-th element, is reported.

The advantages of $MAPbBr_3$ over silicon are (i) The high effective atomic number (Z_{eff}), possible by choosing appropriate components (like Pb), which contributes to enhance the radiation interaction, particularly for X- and γ-rays with energy above 20 keV, where Si starts to be less efficient. (ii) Low production costs, thanks to the material's processability from solution, enable the scalability to large-area devices, making it a cheaper alternative to traditional semi-conductor detectors. The large number of charge carriers produced upon radiation interaction and fast carrier transport properties, characterized by the mobility $\mu \times$ lifetime product $\approx \mathcal{O}(10^{-4})\,\text{cm}^2\,\text{V}^{-1}$ make $MAPbBr_3$ a suitable sensor for radiation detection. Despite these promising characteristics, challenges related to OMHP stability persist, particularly concerning ion migration and the stability of electrical contacts. These instabilities are strongly influenced by the quality of the material, highlighting the importance of improving fabrication processes to enhance the reliability.

Researches on perovskites have initially focused on their use as visible light sensors, exploiting their properties as direct semiconductors. Perovskites are sensitive to light energies just above their band gap (E_g), which can be tuned by varying the elements in the perovskite composition. The PEROV INFN funded project, which aims to characterize $\mathrm{MAPbBr_3}$ as a radiation sensor, addressed earlier studies on perovskite-based light detectors, using 300 nm thick films [3] and very thin crystals (ranging from 2 to 6 µm thick) [4] of $\mathrm{MAPbBr_3}$. Recently, R&D efforts have focused on $\mathrm{MAPbBr_3}$ as X- and γ-ray sensors. However, fewer studies have explored their use in detecting other types of radiation, in particular α-particles [5] or highly ionising protons [6]. Section 2 discusses the detection of Minimum Ionizing Particles (MIPs) by the PEROV INFN project and initial X-ray detection tests. Section 3 outlines future plans within the PEROV project for optimizing $\mathrm{MAPbBr_3}$ sensors for X-ray detection.

2 Bulk single crystal performance

Large single crystals of $\mathrm{MAPbBr_3}$ with dimensions of $O(\mathrm{cm}^3)$ are grown from a solution using the inverse temperature crystallization (ITC) method. Details of the growth process and measured material characterizations are provided in [7].

2.1 Minimum ionising particle detection

A single crystal was tested under a 300 MeV electron beam at the Beam Test Facility (BTF) [8] at the INFN laboratories in Frascati (Italy). The PEROV project has reported for the first detection of a single MIP by a perovskite sensor in [9]. The single crystal sample has an area of 6 mm × 6 mm and is 1.4 mm thick. The perovskite with Indium-Tin Oxide (ITO) contacts on top and bottom to provide the external bias voltage exhibits similar current-voltage (I-V) characteristics regardless of the polarity of the applied voltage. Simulations performed with the GEANT4 software, whose results were presented in the supporting material in [9], show that electrons with this energy behave like MIPs, ionizing along the entire sensor thickness as they pass through and leading to creation of electron-hole pairs which drift towards the electrodes when a bias voltage is applied. The most probable energy deposition is 0.63 MeV, with stochastic fluctuations due to the Landau energy loss. The sensor detects single minimum ionising electrons when a bias voltage of 5 V is applied. It shows a good linearity between the collected signal output voltage and the number of impinging beam electrons. The sensor exhibits good linearity over a dynamic range (i.e. the ratio between the largest and smallest detectable signal in units of impinging beam electrons) of $O(10^3 - 10^4)$, making $\mathrm{MAPbBr_3}$ sensors attractive for dosimetry applications involving high-intensity charged particles. The carrier mobility has been measured to be approximately $\approx 6\,\mathrm{cm^2/V/s}$, which is on the lower end of the literature range, with a corresponding mobility-lifetime product of $3.8 \times 10^{-4}\,\mathrm{cm^2\,V^{-1}}$.

2.2 X-ray detection

$\mathrm{MAPbBr_3}$ is a promising material for X-ray detection above 30 keV due to its high effective atomic number Z_{eff}, high density and low production costs. $\mathrm{MAPbBr_3}$ has a linear attenuation coefficient only partially lower with respect to the CdTe one [10], due to the lower density. The higher production cost of CdTe makes $\mathrm{MAPbBr_3}$ an attractive and viable alternative. A preliminary study on the response of $\mathrm{MAPbBr_3}$ based sensors to X-ray irradiation was conducted with the aim of detecting X-ray with relatively high energy from a conventional laboratory AMPTEK Mini-X tube [11]. The single-crystal used in the measurements described in section 2.1 was exposed to X-rays from the tube with an Ag cathode, operated at 40 kV. The energy spectrum provided by the vendor shows a shoulder of X-rays around 10 keV, along with characteristic lines at 22 keV and 25 keV, as shown in figure 1 (left, black curve). A 2 mm Al filter was used to harden the beam absorbing low-energy photons below approximately 12–15 keV, as visible in figure 1 (left, red curve). Figure 1 (right) shows the corresponding current measured from the single crystal sensor with 2 V bias. The sharp increase around 80 s corresponds to X-rays starting being emitting. The current with (red curve) Al filter diminishes to 10% of the one without (black curve) the Al filter. The current ratio value roughly matches the ratio of the integral of the spectra without and with Al which is roughly 9%; however a full interpretation of the sensor response is not attempted as it depends on the linear attenuation coefficient, the carrier generation and collection efficiency.

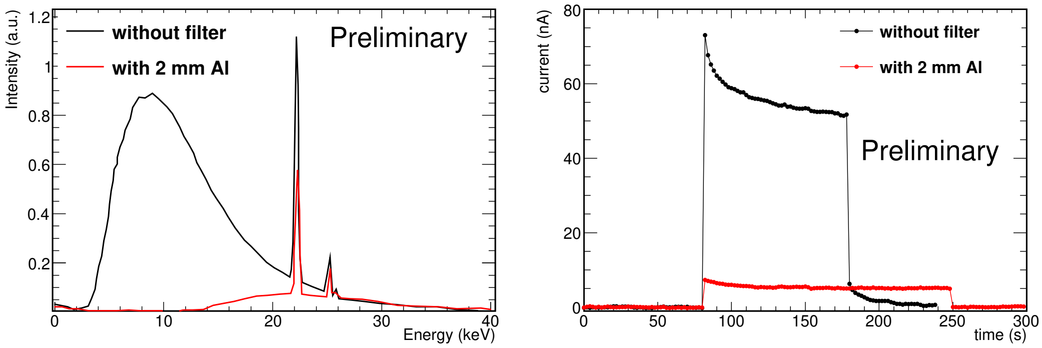

Figure 1. Left: expected X-ray spectrum for an unfiltered (black) and a 2 mm Al-filtered (red) Ag target X-ray tube. Right: single-crystal $\mathrm{MAPbBr_3}$ sensor current response under unfiltered (black) and 2 mm Al-filtered (red) X-ray irradiation. X-rays have been switched on after 80 s for both measurements.

3 Further developments

Perovskite sensors for X-ray and ionizing radiation detection were produced and characterized by the PEROV INFN project. The interests now focus on the development of micropad crystals grown via dewetting techniques on a patterned ITO substrate. Crystal dimensions are 200 × 500 µm, with a thickness ranging from 200 to 500 µm. These smaller crystals are better suited as sensors than single crystals, with a controlled height-to-surface ratio and potential for multi-pixel configurations. For X-ray applications, thinner sensors are advantageous, as X-rays up to 30 keV are absorbed within a few hundred microns. Thicker sensors fail to provide additional signal and increase carrier trapping, reducing efficiency and spatial resolution. The ability to grow perovskite single crystals on patterned surfaces from precursor solutions opens up the possibility of a hybrid assembly, where perovskite crystals are deposited on a thinned chip developed for the ARCADIA project [12], is proposed [13]. The ARCADIA CMOS technology chip is characterized by 50 µm pixel pitch and noise as low as $50\,e^-$ RMS.

Regarding future applications of perovskite sensors as charge particle tracking sensors, a patent was deposited [14] and studies are ongoing to exploit the material high radiation hardness and its self-repair in radiation-harsh environments such as particle beam accelerators or FLASH radiation facilities.

2025 JINST 20 C05028

References

[1] R. Devanathan, L.R. Corrales, F. Gao and W.J. Weber, *Signal variance in gamma-ray detectors — A review*, *Nucl. Instrum. Meth. A* **565** (2006) 637.

[2] S.H. Bennett et al., *Charge transport comparison of FA, MA and Cs lead halide perovskite single crystals for radiation detection*, *Front. Detect. Sci. Technol.* **1** (2023) 1249892.

[3] M. Auf der Maur, F. Matteocci, A. Di Carlo and M. Testa, *Reverse bias breakdown and photocurrent gain in $CH_3NH_3PbBr_3$ films*, *Appl. Phys. Lett.* **120** (2022) 113505.

[4] I. Viola et al., *Microfluidic-Assisted Growth of Perovskite Single Crystals for Photodetectors*, *Adv. Mater. Technol.* **8** (2023) 2300023.

[5] Q. Xu et al., *Detection of charged particles with a methylammonium lead tribromide perovskite single crystal*, *Nucl. Instrum. Meth. A* **848** (2017) 106.

[6] H. Huang et al., *Radiation-Tolerant Proton Detector Based on the MAPbBr3 Single Crystal*, *ACS Appl. Electron. Mater.* **5** (2022) 381.

[7] S. Rizzato, M. Testa and M. Moret, *About crystal growth of hybrid bromide perovskite single crystals*, *J. Cryst. Growth* **653** (2025) 128067.

[8] P. Valente et al., *Linear Accelerator Test Facility at LNF: Conceptual Design Report*, `arXiv:1603.05651`.

[9] M. Testa et al., *Direct detection of minimum ionizing charged particles in a perovskite single crystal detector with single particle sensitivity*, *Nanoscale* **16** (2024) 12918.

[10] NIST database, https://physics.nist.gov/PhysRefData/Xcom/html/xcom1.html.

[11] Amptek, https://www.amptek.com/products/mini-x2-x-ray-tube.

[12] ARCADIA collaboration, *Sensor Design Optimization of Innovative Low-Power, Large Area FD-MAPS for HEP and Applied Science*, *Front. in Phys.* **9** (2021) 625401 [`arXiv:2011.09723`].

[13] L. Pancheri, M. Testa and I. Viola, *HyPoSiCX = Hybrid Perovskite on Silicon CMOS X-ray Detectors*, Italian PRIN 2022 project granted.

[14] Patent IT 102023000012477, https://web.infn.it/TechTransfer/?portfolio_page=p23-025.

2025 JINST 20 C05028